A Meshless Method for Some Inverse Problems Associated with the Helmholtz Equation

Bangti Jin [a,b], Yao Zheng [a,c,*]

[a] *Center for Engineering and Scientific Computation, Zhejiang University, Hangzhou, Zhejiang, 310027, P.R. China*

[b] *Department of Mathematics, Zhejiang University, Hangzhou, Zhejiang, 310027, P.R. China*

[c] *College of Computer Science, Zhejiang University, Hangzhou, Zhejiang, 310027, P.R. China*

Abstract

In this paper, a new numerical scheme based on the method of fundamental solutions is proposed for the numerical solution of some inverse boundary value problems associated with the Helmholtz equation, including the Cauchy problem. Since the resulting matrix equation is badly ill-conditioned, a regularized solution is obtained by employing truncated singular value decomposition, while the regularization parameter for the regularization method is provided by the L-curve method. Numerical results are presented for problems on smooth and piecewise smooth domains with both exact and noisy data, and the convergence and stability of the scheme are investigated. These results show that the proposed scheme is highly accurate, computationally efficient, stable with respect to the noise in the data and convergent with respect to decreasing the amount of data noise and increasing the distance between the physical and fictitious boundaries, and could be considered as a competitive alternative to existing methods for these problems.

Key words: The method of fundamental solutions; Cauchy problem; Helmholtz equation; Truncated singular value decomposition; Inverse problem

* Corresponding author. Tel.: 86-571-8795-3168; fax: 86-571-8795-3167.
 Email address: `yao.zheng@zju.edu.cn` (Yao Zheng).

1 Introduction

The Helmholtz equation arises naturally in many scientific and engineering areas. It is frequently used for analyzing acoustics, wave propagation and scattering [1], vibration of membranes and other structures, electromagnetic field, and heat conduction in fins [2].

With boundary conditions specified on the entire boundary of the solution domain, this constitutes the forward problem for the Helmholtz equation, which has been studied extensively in the past years. Unfortunately, in many scientific and engineering contexts, the boundary conditions are not completely known, due to technical difficulties associated with data acquisition. For example, a part of the boundary is inaccessible to direct measurement, and the presence of measuring devices, such as sensors, will disturb the process under investigation, thus only incorrect data can be collected. To fully determine the process, additional data must be supplied, either other boundary conditions on the same accessible part of boundary or measurements at some internal points in the domain. The task is to determine the boundary conditions on the inaccessible part of the boundary with the assistance of the additionally supplied data. These are examples of inverse problems, including the Cauchy problem as a particular case, and it is well-known that they are ill-posed in the sense that small perturbations in the data may result in an enormous deviation in the solution. Therefore an accurate and stable solution of inverse problems is much more difficult to obtain than that of the forward problem.

Several numerical methods have been proposed for the Cauchy problem [3–8]. Roughly speaking, these methods can be classified into iterative and direct methods. In iterative methods [7,8], one starts with an initial guess of the boundary condition, and adjusts it iteratively by minimizing certain functionals such as error between the calculated data and measured data. It could be extremely time-consuming since a forward problem has to be solved at each iteration step. In the direct methods, it takes much less computation time since one has to discretize the problem only for one time, but it may suffer from numerical instability.

In the present paper, we propose a new numerical scheme for solving the inverse problems for the Helmholtz equation directly. It is based on the method of fundamental solutions, which is a truly meshless boundary-type technique for the solution of partial differential equations. It should be mentioned that similar ideas have been developed by Marin and Lesnic [9,10]. Several numerical examples are given to demonstrate the efficiency of the proposed scheme.

The paper is organized in six sections. In Section 2, we formulate the problem mathematically. The two sections following are devoted to the numerical algo-

rithm. The method of fundamental solutions is described in Section 3, while regularization techniques with rules for choosing an appropriate regularization parameter are described in Section 4. In Section 5, we present results for five numerical examples on domains with both smooth and non-smooth geometry. Finally, concluding remarks are given in Section 6.

2   Mathematical formulation of the problem

Let Ω be an open bounded domain in $\mathbf{R}^d$, where d is the dimensionality of the space, and $\Gamma = \partial\Omega$ its boundary. Then the mathematical formulation of the problem can be written as

$$(\Delta + k^2)u(\mathbf{x}) = 0, \ \mathbf{x} \in \Omega, \tag{1}$$

where Δ is the Laplace operator, and k is a complex number known as a wave number. For the case that k is purely imaginary, i.e., $k = i\lambda, \ i = \sqrt{-1}$, the equation is also known as the modified Helmholtz equation. It can be used to model heat conduction in a fin [2]. To eliminate the imaginary unit, Eq. (1) may be rewritten as

$$(\Delta - \lambda^2)u(\mathbf{x}) = 0, \ \mathbf{x} \in \Omega. \tag{2}$$

In this paper, we consider only the cases that k is real and purely imaginary, and for the ease of presentation, they are respectively denoted the Helmholtz equation and modified Helmholtz equation hereafter.

Let $n(\mathbf{x})$ be the unit outward normal vector on the boundary Γ, and $\phi(\mathbf{x})$ the flux at a point $\mathbf{x} \in \Gamma$

$$\phi(\mathbf{x}) = \frac{\partial u(\mathbf{x})}{\partial n}, \ \mathbf{x} \in \Gamma. \tag{3}$$

Now the boundary condition is not known on the complete boundary Γ but only on a part of it

$$\mathcal{B}_1 u(\mathbf{x}) = f(\mathbf{x}), \ \mathbf{x} \in \Gamma_1, \tag{4}$$

where Γ_1 is the accessible part of the boundary Γ, and $\mathcal{B}_1$ is a linear boundary operator prescribing boundary conditions.

This problem is mathematically under-determined and additional data must be supplied to fully determine it. According to the types of the additional data, there are two possible formulations of the problem.

Formulation 1. The additional data is another type of boundary condition specified on the same accessible part of the boundary, but different from that given by Eq. (4),

$$\mathcal{B}_2 u(\mathbf{x}) = g(\mathbf{x}), \ \mathbf{x} \in \Gamma_1, \tag{5}$$

where $\mathcal{B}_2$ is a linear boundary operator different from $\mathcal{B}_1$. It may be available only at a few points on Γ_1.

Formulation 2. The additional data is measurements at some internal points

$$\mathcal{D}u(\mathbf{x}_i) = h(\mathbf{x}_i), \ \mathbf{x}_i \in \Omega, \ i = 1, 2, \ldots, n_a, \tag{6}$$

where $\mathcal{D}$ is a data functional dictating the measured quantities, and n_a is the total number of internal measuring points.

In Formulation 1, the part of boundary Γ_1 is over-specified since both types of boundary conditions are specified, and in this case, the problem is also known as the Cauchy problem for the Helmholtz equation, which is notorious for its ill-posedness. In this paper, we give results only for Formulation 1, however, similar results can be obtain for Formulation 2.

3 The method of fundamental solutions

In both iterative and direct methods, the governing differential equation must be discretized. There are several ways to achieve this, notably the finite difference method (FDM), finite element method (FEM), finite volume method (FVM), and boundary element method (BEM). The first three require a mesh on the domain to support the solution process, however, generating a good quality mesh for complicated geometry could be extremely time-consuming. The BEM reduces the dimensionality of the problem by one, thus it alleviates partly the difficulty, and it is popular in recent years. Despite its popularity, there are still problems with it. It requires the evaluation of singular integrals for using singular fundamental solutions, and generating a good quality mesh for the boundary of complex geometry in higher dimensions is still nontrivial. Meshless methods receive much attention from both scientific and engineering community in recent years due to their meshless characteristics. Amongst meshless methods, there are element free-Galerkin method (EFGM) [11], H-p cloud [12], reproducing kernel particle method (RKPM) [13], meshless local Petrov-Galerkin (MLPG) method [14], Kansa's method [15], the method of fundamental solutions [16,17] etc. Here we use the method of fundamental solutions to discretize the Helmholtz equation.

The method of fundamental solutions (MFS) is a truly meshless boundary-type collocation technique for discretizing partial differential equations. It approximates the solution of a partial differential equation by a linear combination of fundamental solutions with singularities, also known as source points, located on a fictitious boundary outside of the solution domain. For theoretical grounds of the method, we refer to the comprehensive surveys [16,17] and references therein, and for recent developments, we refer to Refs. [18–20].

The fundamental solution $u^*(\mathbf{x})$ of the modified Helmholtz equation in $\mathbf{R}^d$ is given by [21]

$$u^*(\mathbf{x}) = \begin{cases} \frac{1}{2\pi} K_0(\lambda r), \ \mathbf{x} \in \mathbf{R}^2, \\ \frac{1}{4\pi r} e^{-\lambda r}, \quad \mathbf{x} \in \mathbf{R}^3, \end{cases} \tag{7}$$

and for the Helmholtz equation, it is given by

$$u^*(\mathbf{x}) = \begin{cases} \frac{1}{2\pi} Y_0(kr), \ \mathbf{x} \in \mathbf{R}^2, \\ \frac{1}{4\pi r} e^{-ikr}, \ \mathbf{x} \in \mathbf{R}^3, \end{cases} \tag{8}$$

where $r = \|\mathbf{x}\|_2$, $\|\cdot\|_2$ is the Euclidean norm on $\mathbf{R}^d$, and K_0 and Y_0 denote the modified Bessel and Bessel function of the second kind of order zero, respectively. Note that the fundamental solution to the differential operator is not unique. For the Helmholtz equation, we may take the Hankel function as the fundamental solution, and similar results can be obtained.

In the MFS, we seek an approximate solution by

$$u(\mathbf{x}) = \sum_{j=1}^{n_s} a_j G_j(\mathbf{x}), \text{ for } \mathbf{x} \in \Omega, \tag{9}$$

where $G_j(\mathbf{x}) = u^*(\mathbf{x} - \mathbf{y}_j)$, $\{\mathbf{y}_j\}$ are the source points located on a fictitious boundary outside of the solution domain, n_s is the number of source points, and $\{a_j\}$ are the unknown coefficients to be determined.

Although the approximate solution $u(\mathbf{x})$ satisfies the differential equation automatically, it does not necessarily satisfy the boundary conditions and the additional data. The latter can be achieved by means of the collocation method. Let $\{\mathbf{x}_i\}$ be a set of points chosen on the accessible part of the boundary. By collocating Eqs. (4) and (5) at $\{\mathbf{x}_i\}$, we arrive at following system of linear algebraic equations

$$f(\mathbf{x}_i) = \sum_{j=1}^{n_s} a_j \mathcal{B}_1 G_j(\mathbf{x}_i), \ i = 1, 2, \ldots, n_b, \tag{10}$$

$$g(\mathbf{x}_i) = \sum_{j=1}^{n_s} a_j \mathcal{B}_2 G_j(\mathbf{x}_i), \ i = n_b + 1, \ldots, n_b + n_a, \tag{11}$$

for Formulation 1, where n_b and n_a are the number of collocation points on Γ_1 for the boundary conditions defined by $\mathcal{B}_1$ and $\mathcal{B}_2$, respectively. In a similar manner, analogous formulae can be obtained for Formulation 2.

In brevity, we have the following matrix equation for Formulation 1

$$\mathbf{A}\mathbf{a} = \mathbf{b}, \tag{12}$$

5

where $\mathbf{A} = (A_{ij})$ is an interpolation matrix, $\mathbf{a} = (a_1, a_2, \ldots, a_{n_s})^T$ is a coefficient vector, $n = n_b + n_a$, and $\mathbf{b} = (f(\mathbf{x}_1), f(\mathbf{x}_2), \ldots, f(\mathbf{x}_{n_b}), g(\mathbf{x}_{n_b+1}), \ldots, g(\mathbf{x}_n))^T$ is a data vector. Moreover, the entries A_{ij} of the interpolation matrix $\mathbf{A}$ are defined by

$$A_{ij} = \begin{cases} \mathcal{B}_1 G_j(\mathbf{x}_i), \ i = 1, 2, \ldots, n_b, \ j = 1, 2, \ldots, n_s, \\ \mathcal{B}_2 G_j(\mathbf{x}_i), \ i = n_b + 1, \ldots, n, \ j = 1, 2, \ldots, n_s. \end{cases} \tag{13}$$

The resulting matrix equation (12) is often severely ill-conditioned. Its accurate and stable solution is very important for obtaining physically meaningful numerical results, which will be discussed in further detail in the next section.

To implement the method, there remains one thing to be determined, i.e., the placement of the source points. There are two approaches to determine the source points: static and dynamic. In the static approach, the source points are pre-assigned and kept fixed through the solution process, while in the dynamic approach source points are determined simultaneously with the coefficients during the solution process [17]. The dynamic approach results in a system of nonlinear equations, which may be solve using minimization methods. However, the discretized problem is highly ill-posed. In other words, the dynamic approach transforms the problem into a more difficult nonlinear ill-posed problem. Thus from a computational point of view, the dynamic approach may not be appropriate, and this is especially true for inverse problems with noisy data. Recently, Mitic and Rashed [22] show that the distribution of source points is not important under minor conditions. Thus the dynamic approach for determining the optimal location of the source points might be unnecessary, and we employ the static approach in our computations.

4 Regularization techniques

One difficulty with the MFS is that the condition number of the interpolation matrix is extremely large, as observed by Kitagawa [23,24], Golberg and Chen [16]. The MFS can be regarded as a Fredholm integral equation of the first kind [16], which is severely ill-posed according to the theory of integral equations [25]. Consequently, as an approximation to the integral operator, the interpolation matrix is highly ill-conditioned. For the solution of forward problems, this does not pose great challenges, since the known data are exact. Standard methods, such as the Gauss elimination, the LU factorization and the least squares method, could yield accurate results.

However, for inverse problems, the situation is delicate. Inverse problems are usually ill-posed, and the ill-posedness carries over to the discrete ones – the

resulting matrix equations. Undoubtedly this will make the matrix equations more ill-conditioned. The thing that really complicates the situation is that the available data for inverse problems is measured and inevitably contaminated by measurement errors. Thus the bad conditioning with the interpolation matrix can be disastrous. Standard methods may fail to yield satisfactory results due to the ill-conditioning with $\mathbf{A}$ and the presence of data noise.

Regularization methods are powerful and efficient tools for accurately and stably solving ill-posed problems. In our computations we use the truncated singular value decomposition (TSVD) [26] to solve the matrix equation arising from the MFS. Other regularization methods [27], such as the Tikhonov regularization method, could be considered, and similar results can be obtained, but these will not be further pursued in this paper.

In the singular value decomposition (SVD), a matrix $\mathbf{A} \in \mathbf{R}^{m \times n}(m \geq n)$ is decomposed into

$$\mathbf{A} = \mathbf{U}\mathbf{\Sigma}\mathbf{V}^T, \tag{14}$$

where $\mathbf{U} = [\mathbf{u}_1, \mathbf{u}_2, \ldots, \mathbf{u}_m]$ and $\mathbf{V} = [\mathbf{v}_1, \mathbf{v}_2, \ldots, \mathbf{v}_n]$ are column orthonormal matrices, with column vectors called left and right singular vectors, respectively, T denotes the matrix transposition, and $\mathbf{\Sigma} = \mathrm{diag}(\sigma_1, \sigma_2, \ldots, \sigma_n)$ is a diagonal matrix with nonnegative diagonal elements in non-increasing order, which are the singular values of $\mathbf{A}$.

A convenient measure of the conditioning of the interpolation matrix $\mathbf{A}$ is the condition number $Cond$ defined as bellow

$$Cond = \frac{\sigma_1}{\sigma_n}. \tag{15}$$

By means of the SVD, the solution $\mathbf{a}^0$ to Eq. (12) can be succinctly written as a linear combination of right singular vectors

$$\mathbf{a}^0 = \sum_{i=0}^{k} \frac{\mathbf{u}_i^T \mathbf{b}}{\sigma_i} \mathbf{v}_i, \tag{16}$$

where k is the rank of $\mathbf{A}$. For a rectangular matrix, the solution given by Eq. (16) is the least squares solution. For an ill-conditioned matrix equation, there are small singular values, the least squares solution is dominated by the contributions from small singular values, and therefore it becomes unbounded and oscillatory. One simple remedy to the difficulty is to leave out small singular values, i.e., by considering an approximate solution, $\mathbf{a}^p$, defined by

$$\mathbf{a}^p = \sum_{i=1}^{p} \frac{\mathbf{u}_i^T \mathbf{b}}{\sigma_i} \mathbf{v}_i, \tag{17}$$

where $p \leq k$ is the regularization parameter, which determines when one

starts to leave out small singular values. Note that if $p = k$, the approximate solution is the exact solution. This method is known as truncated singular value decomposition [26] in the inverse problem community.

The SVD has been used to analyze the MFS for the Laplace equation with exact data [28] and the Laplace and biharmonic equations subjected to noisy boundary data [29]. It was established that the accuracy of numerical solutions is relatively independent of the location of the source points when using the TSVD to solve matrix equations arising from the MFS.

The performance of regularization methods depends to a great deal on suitable choice of regularization parameter. If a reliable estimate of the amount of data noise is available, deterministic approaches such as the discrepancy principle can work effectively. In case of no *a priori* information, heuristic approaches, such as L-curve method [30,31] and generalized cross validation [32], are more preferable. In this paper, we employ the L-curve method to determine the regularization parameter for the TSVD. The L-curve method was first used by Lawson and Hansen [33], and later popularized by Hansen et al [30,31].

Define the following curve

$$L = \left\{ \left(\log(\|\mathbf{a}^i\|_2), \log(\|\mathbf{A}\mathbf{a}^i - \mathbf{b}\|_2) \right), \ i = 1, 2, \ldots, k \right\}. \tag{18}$$

The curve is known as L-curve since it is typically of L-shape. The regularization parameter corresponding to the corner of the L-curve is taken as a final regularization parameter, since at the corner a good tradeoff between the residual and solution norm is achieved. The L-curve is robust and stable with respect to both uncorrelated and highly correlated noise, and it usually works effectively with practical problems. However, there are theoretical results disfavor the L-curve, and for the details we refer to Refs. [34,35].

5 Numerical experiments

In this section we present the numerical results obtained by the general numerical scheme described in previous sections, namely the MFS in conjunction with the TSVD. The effect of regularization is discussed, and the convergence and stability with respect to data noise are investigated. All computations are carried out on a PC with 1.8GHz CPU and 512MB RAM.

5.1 Numerical examples

The domains under consideration are a circular domain $\Omega = \{(x_1, x_2) | x_1^2 + x_2^2 < 1\}$, an annular domain $\tilde{\Omega} = \{(x_1, x_2) | 0.25 < x_1^2 + x_2^2 < 1\}$, and a domain $\hat{\Omega}$ with a complicated geometry as schematically shown in Fig. 2(a). The boundary of each domain is divided into two disjointed parts, i.e., the accessible part Γ_1 and the inaccessible part Γ_2. For Ω, $\Gamma_1 = \{(r, \theta) | r = 1, 0 \le \theta < \pi\}$ and $\Gamma_2 = \{(r, \theta) | r = 1, \pi \le \theta < 2\pi\}$, where (r, θ) is the plane polar coordinate. For $\tilde{\Omega}$, $\Gamma_1 = \{(x_1, x_2) | x_1^2 + x_2^2 = 1\}$ and $\Gamma_2 = \{(x_1, x_2) | x_1^2 + x_2^2 = 0.25\}$. For $\hat{\Omega}$, these two parts of boundary are shown in Fig. 2(b). For the convenience of comparison and illustration of accuracy of the method, we consider following analytical solutions.

Example 1. This example is the modified Helmholtz equation on Ω, with $\lambda = 1$. The analytical solution $u(\mathbf{x})$ is taken to be

$$u(\mathbf{x}) = \exp\left(\frac{1}{2}x_1 + \frac{\sqrt{3}}{2}x_2\right), \quad \mathbf{x} = (x_1, x_2) \in \Omega.$$

Example 2. This example is the Helmholtz equation on Ω, with $k = 1$. The analytical solution $u(\mathbf{x})$ is taken to be

$$u(\mathbf{x}) = \sin(x_1) + \cos(x_2), \quad \mathbf{x} = (x_1, x_2) \in \Omega.$$

Example 3. This example is the modified Helmholtz equation on $\hat{\Omega}$, with $\lambda = \sqrt{2}$. The analytical solution $u(\mathbf{x})$ is taken as

$$u(\mathbf{x}) = \exp\left(x_1 + x_2\right), \quad \mathbf{x} = (x_1, x_2) \in \hat{\Omega}.$$

Example 4. This example is the Helmholtz equation on $\hat{\Omega}$, with $k = 1$. The analytical solution $u(\mathbf{x})$ is taken to be

$$u(\mathbf{x}) = \sin(\sqrt{2}x_1)\sinh(x_2) + \cos(x_2), \quad \mathbf{x} = (x_1, x_2) \in \hat{\Omega}.$$

Example 5. This example is the modified Helmholtz equation on the doubly connected domain $\tilde{\Omega}$, with $\lambda = 2$. The analytical solution $u(\mathbf{x})$ is taken as

$$u(\mathbf{x}) = \exp\left(x_1 - \sqrt{3}x_2\right), \mathbf{x} = (x_1, x_2) \in \tilde{\Omega}.$$

Example 1 is taken from Marin et al. [7], with slight modifications indicated below. Examples 1 and 2 are adopted to illustrate the efficiency of the scheme for smooth geometry, while Examples 3 and 4 for nonsmooth geometry. Note

9

that $\hat{\Omega}$ involves sharp notches and corners, which is deliberately designed to verify the robustness, efficiency and effectiveness of the proposed scheme when dealing with problems with arbitrarily complicated geometry. Example 5 is adopted to illustrate the difficulty with the scheme for multi-connected domains.

In this paper, we consider only Formulation 1, i.e., the Cauchy problem. Without loss of generality, the boundary conditions defined by $\mathcal{B}_1$ and $\mathcal{B}_2$ are respectively taken to be the Dirichlet and Neumann boundary conditions unless otherwise specified. For the results presented below, the source points are distributed evenly on a circle surrounding the solution domain, and the radius of the circles is taken to be 3. Such placement is optimal for a circular domain [36]. The number of source points is 20 unless otherwise specified. The number of collocation points on the accessible part of boundary Γ_1 is 20 for Ω and $\tilde{\Omega}$, and is 24 for $\hat{\Omega}$. The collocation points on Γ_1 are used for both types of boundary conditions. The diagrams of the boundary, boundary collocation points and source points for the Ω and $\tilde{\Omega}$ are schematically shown in Fig. 1(a) and 1(b), respectively, while for $\hat{\Omega}$ it is shown in Fig. 2(b).

For practical problems, the available data is usually contaminated by measurement errors, and the stability of the numerical method is of vital importance for obtaining physically meaningful results. In order to investigate the stability of the scheme with respect to data noise, we use simulated noisy data generated by the following formula

$$\tilde{b}_i = b_i(1 + \varepsilon\zeta), \ i = 1, 2, \ldots, n, \tag{19}$$

where ζ is a normally distributed random variable with zero mean and unit standard deviation, and ε is the level of data noise. In our computations, the random variable ζ is realized by using Matlab function `randn()`.

In order to measure the accuracy of the numerical approximation $\tilde{f}$ with respect to the exact solution f, we use the relative error $rel(f)$ defined by

$$rel(f) = \frac{\sqrt{\sum_{i=1}^{N}(\tilde{f}_i - f_i)^2}}{\sqrt{\sum_{i=1}^{N} f_i^2}} \tag{20}$$

where $\tilde{f}_i$ and f_i are the numerical and exact solutions evaluated at a point $\mathbf{x}_i \in \Gamma_2$, respectively. Here N is the total number of collocation points on Γ_2 at which the solutions are evaluated, and it is taken to be 40 for the results presented below.

Before proceeding to the numerical results by regularization methods, it is worth studying how the regularization method improves the accuracy of the numerical results. To do this, we consider Example 1 with 1% data noise. The condition number of the interpolation matrix $\mathbf{A}$ for this example is 5.79×10^6, which is large compared with the size of $\mathbf{A}$, i.e., 40×20.

The results obtained by the least squares method are shown in Fig. 3(a), where the solid and dotted curves represent the analytical and numerical solutions, respectively. The least squares solution is highly oscillatory, and it could not be used as an approximate solution at all. It's noted that the Gaussian elimination and the LU factorization yield similar results in case of square interpolation matrices. Thus standard methods could not yield accurate results for noisy data.

The trouble with the least squares method is that the solution is dominated by the contributions from small singular values. There are a lot of small singular values in the singular value spectrum of $\mathbf{A}$, which is shown in Fig. 4(a). Furthermore, the singular values decay gradually to zero without any obvious gap, and eventually cluster at zero. This is typical for matrices arising from Fredholm integral equations of the first kind [30,31], to which the MFS is mathematically equivalent.

The L-curve for Example 1 with 1% noise is shown in Fig. 4(b). The curve approximately consists of two parts: horizontal and vertical, which correspond to under-regularization and over-regularization, respectively. At the corner of the curve, a good tradeoff between the solution and residual norms is achieved, and we take the regularization parameter corresponding to the corner as the final regularization parameter. For the present example, the regularization parameter given by the L-curve method is $p = 9$.

The numerical results by the TSVD are shown in Fig. 3(b). From the figure, the TSVD could yield very accurate results for noisy data. Therefore, the regularization method is indispensable to guarantee the stability and accuracy of the proposed scheme for noisy data. The regularization method restores the stability by filtering out the contributions from data noise effectively without losing too much information. The numerical results also indicate that the L-curve method provides an appropriate regularization parameter for the TSVD.

5.3 Convergence analysis

It is well-known that the accuracy of the MFS depends to a great deal on the distance between the physical and fictitious boundary outside of the solution domain. For forward problems with exact data, it's generally advised taking the fictitious boundary as far away from the physical domain as possible, as much as the machine accuracy allows. Ramachandran [28] showed that the singular value decomposition can mitigate the critical dependence, which is also the case for forward problems with noisy data [29]. In the sequel, we investigate the convergence of method with respect to increasing the radius R of the circle where the source points are distributed.

In Fig. 5, we give the results for Example 1 with the source points distributed evenly on a circle with various values of the radius R, where $rel(u)$ and $rel(\phi)$ are the relative error for the retrieved Dirichlet and Neumann boundary conditions, respectively. The regularization parameter is 13 for $R = 1.5$, 16 for the radius R between 2.0 and 4.5, 17 for the radius R between 5.0 and 8.5, and 19 for the rest. The condition number increases steadily with the increase of the source radius. The accuracy of the numerical results improves as the radius R increases, however, it then tends to level off. Although not presented in the Fig. 5, it is reported that the least squares method fails to work for small values of the radius R, e.g. $R = 1.5$, while the TSVD yields very accurate numerical results even in this case. For large values of the radius R, the improvement in accuracy is not so impressive. A very large value of the radius R is generally not advised due to the severe ill-conditioning and the presence of rounding errors inherent to all numerical computations, which will eventually take effect.

For noisy data, we present only the results by the TSVD. The results for Example 1 with 1% noise using various values of the radius R are shown in Fig. 6(a), where the regularization parameter p is 9 for all values of the radius R. The accuracy of the numerical results is practically the same for the radius R from 3 to 40, and it's relatively independent of R. It has been established for forward problems subjected to noisy boundary data [29].

Next we investigate the convergence of the numerical results with respect to the number of source points n_s. The results for Example 1 using various number of source points are shown in Fig. 7, where the regularization parameter p for the TSVD is taken to be 4, 8, 16, 20, 22, 28 and 28, respectively. The accuracy of numerical results improves as n_s increases, and the TSVD can improve the accuracy by several orders in magnitude. The method is exponentially convergent with respect to increasing n_s. The results for Example 1 with noisy data are shown in Fig. 6(b). The regularization parameter p is 4 for $n_s = 5$, 8 for $n_s = 10$, and 9 for other n_s. It is found that the accuracy of

the numerical results is practically the same for n_s from 10 to 40.

5.4   Numerical results and discussions

In this part, we discuss the results for the numerical examples, for both exact and noisy data. One numerically difficult case is also considered.

For exact data, the method could be extremely accurate. To illustrate this point, we give the error between the numerical solution by the TSVD with $p = 16$ and analytical solution for Example 1 with exact data, which is shown in Fig. 8. The maximum error for the retrieved Dirichlet and Neumann boundary conditions is less than 6×10^{-7} and 2×10^{-6}, respectively.

The striking accuracy is due to the spectral convergence property of the MFS [16,36]. Thus a few collocation points are sufficient to yield accurate results, and the size of resulting system of linear equations is quite small. Therefore the method is computationally very efficient. To achieve the same accuracy by the FEM, FDM or BEM, the corresponding mesh used must be very fine, which undoubtedly would increase the computation time considerably.

The numerical results for Example 1 with various levels of data noise are presented in Fig. 9. Even with a large amount of noise ($\varepsilon = 2\%$) incorporated in the data, the results still agree quite well with the analytical solution, and the numerical solution converges to the analytical solution as the amount of data noise decreases. The observation could also be drawn from the numerical results for Example 2, which are shown in Fig. 10. The accuracy for these two examples with 2% noise is shown in Table 1, where p is the regularization parameter given by the L-curve method.

Example 1 has been solved by Marin et al. [7] using a BEM implementation of the alternating iterative method due to Kozlov et al. [37], which reduces the problem to solving a sequence of well-posed forward boundary value problems. However, the accessible part boundary Γ_1 considered there is larger than that in the present study. Since Marin et al. [7] did not give the formula used to generate simulated noisy data, we could not compare the results thoroughly. However, a preliminary comparison with the results of Marin et al. [7] shows that the results presented here seem to be more accurate for both exact and noisy data. Furthermore, the alternating iterative algorithm requires many iterations to achieve an acceptable accuracy, and at each iteration, a forward problem must be solved, hence it is computationally more expensive compared with the proposed scheme.

The scheme works equally well for problems with non-smooth geometry. To illustrate this point, we consider examples with complex geometry, i.e., Exam-

ples 3 and 4. The numerical results for Examples 3 and 4 with various levels of data noise are presented in Fig. 11 and 12, respectively. From Table 1, the accuracy achieved for these two examples is comparable with that for smooth geometry. This shows clearly the facility of the method for problems with complicated geometry, which is especially important for higher-dimensional problems, since generating a good quality mesh for complicated geometry in higher dimensions could be extremely time-consuming.

For problems with informal boundary conditions, such as the oblique boundary condition, it is generally difficult to deal with using traditional methods, such as the FEM and BEM. However, no additional difficulty would arise for the proposed scheme. As an example, we consider Example 3 again with one slight modification, i.e., the Neumann condition on the parts of boundary non-parallel to axes (Γ_3 and Γ_4 in Fig. 2(a)) is replaced by

$$\frac{\partial u(x)}{\partial \tau} = h(x),$$

where τ is a unit vector, which may vary in terms of position. In the present study, τ is taken to be $\left(\frac{\sqrt{2}}{2}, \frac{\sqrt{2}}{2}\right)$ on Γ_3, and $\left(\frac{\sqrt{2}}{2}, -\frac{\sqrt{2}}{2}\right)$ on Γ_4, respectively. The numerical results for the modified version of Example 3 are presented in Fig. 13. The accuracy of the numerical results is the same as that for Example 3. This shows clearly the facility of the proposed scheme for problems with complicated boundary conditions.

It is especially stressed that the coding effort for these more complicated cases makes no difference for the proposed scheme. Note that for problems with more complicated geometry or boundary conditions, the analytical solution is smooth. For the case that the solution is non-smooth, it could be far more involved, and it is beyond the scope of present study.

Till now we have considered only singly connected domains. We now turn to multi-connected case, i.e., Example 5. For multi-connected domain, the source points can be placed outside and inside the hole, and they can also be placed as singly connected domain [38]. In this paper, we investigate both approaches. The results for exact data are shown in Table 2, where n_o and n_i are the numbers of source points evenly distributed on circles outside with $R = 3$ and inside the hole with $R = 0.2$, respectively. From Table 2, the placement of source points has significant effect on the accuracy of the numerical results. When n_s is fixed at 20, the accuracy of the numerical results deteriorates as the number of source points inside the hole increases. In fact, when n_i increases to 10, the numerical results fail to converge. On the other hand, when n_o is fixed at 20, the accuracy of the numerical results deteriorates as n_i increases. Therefore the most accurate numerical results were obtained when all the source points are place outside of the domain.

For noisy data, the results are shown in Table 3. From the table, the placement of source points has a more severe effect in the presence of data noise. As n_i exceeds a certain number, the MFS coupled with TSVD fails to yield satisfactory results. It is observed that increasing the number of source point inside the hole would deteriorate the accuracy of the numerical results. Thus the placement of the source points could be quite tricky for multi-connected domains, and an inappropriate placement will lead to erroneous results. We present the numerical results for Example 5 using only 20 source points outside the solution domain in Fig. 14. With up to 2% noise in the data, the retrieved Dirichlet and Neumann boundary conditions are both in excellent agreement with the exact ones.

From Table 1, the accuracy achieved for all the examples is comparable, which demonstrates the efficacy of the scheme consistently. Note that the errors in the Neumann boundary condition are larger than that in the Dirichlet boundary condition, usually by one order in magnitude. This is not out of expectation, since the latter involves the derivative of the solution.

From the numerical verification demonstrated above, it could be concluded that the proposed scheme is highly accurate, computationally efficient, stable with respect to data noise, convergent with respect to decreasing the amount of data noise and increase the distance between the physical and fictitious boundaries, and versatile for problems on singly-connected domains with complicated geometry or (and) complicated boundary conditions. Furthermore, the approximation of the solution and its derivative on the entire solution domain is readily available by simple and direct function evaluation. In comparison with existing methods for this problem, the proposed scheme could be a competitive alternative.

6   Conclusions

In the paper, an efficient and stable numerical scheme for some inverse problems associated with the Helmholtz equation is proposed. The scheme is based on the method of fundamental solutions in combination with a popular regularization method – truncated singular value decomposition. Moreover, the selection of an appropriate regularization parameter has been discussed. Numerical results for examples with both smooth geometry and non-smooth geometry, as well as singly connected and multi-connected domains, are presented, and comparisons are made with results reported in the literature. The results show that the proposed scheme can be a competitive alternative to existing methods for the problems.

There are several potential extensions of the proposed scheme, which is cur-

rently under investigation in our group. Firstly, although this paper considers only problems in the two-dimensional space, the scheme is readily extended to problems in higher dimensions. Secondly, the proposed scheme applies also to ill-posed Cauchy problems associated with other elliptic partial differential equations, as long as the fundamental solution of the differential operator is known. Thirdly, combined with the now mature numerical technique – the dual reciprocity method [39] and radial basis functions, we can extend the scheme to a much wide class of non-homogeneous problems.

For large-scale problems, the general numerical scheme, namely the MFS in conjunction with the TSVD, is of limited use, since computing singular value decomposition for large-scale matrices is prohibitive to use. A promising alternative is to use iterative regularization methods, such as conjugate gradient type methods and GMRES [40], where the computation-intensive step at each iteration, namely matrix-vector multiplication, could be greatly accelerated using the fast multipole method [41].

Acknowledgements

References

[1] G.M.L. Gladwell, N.B. Willms, On the mode shapes of the Helmholtz equation, J. Sound Vib. 188(1995) 419-433.

[2] A.S. Wood, G.E. Tupholme, M.I.H. Bhatti, P.J. Heggs, Steady-state heat transfer through extended plane surfaces, Int. Comm. Heat Mass Transfer 22(1995) 99-109.

[3] M.R. Bai, Application of BEM (boundary element method)-based acoustic holography to radiation analysis of sound sources with arbitrarily shaped geometries, J. Acoust. Soc. Am. 92(1992) 533-549.

[4] Z. Wang, S.F. Wu, Helmholtz equation least-squares method for reconstructing the acoustic pressure field, J. Acoust. Soc. Am. 102(1997) 2020-2032.

[5] S.F. Wu, J. Yu, Reconstructing interior acoustic pressure fields via Helmholtz equation-least-squares method, J. Acoust. Soc. Am. 104(1998) 2054-2060.

[6] V. Isakov, S.F. Wu, On theory and application of the Helmholtz equation least squares method in inverse acoustics, Inv. Prob. 18(2002) 1147-1159.

[7] L. Marin, L. Elliott, P.J. Heggs, D.B. Ingham, D. Lesnic, X.Wen, An alternating iterative algorithm for the Cauchy problem associated to the Helmholtz equation, Comput. Meth. Appl. Mech. Engrg. 192(2003) 709-722.

[8] Y.A. Gryazin, M.V. Klibanov, T.R. Lucas, Two numerical methods for an inverse problem for the 2-D Helmholtz equation, J. Comput. Phys. 184(2003) 122-148.

[9] L. Marin, D. Lesnic, The method of fundamental solutions for the Cauchy problem associated with two-dimensional Helmholtz-type equations, Comput. Struct. 83(2005) 267-278.

[10] L. Marin, D. Lesnic, A meshless method for the numerical solution of the Cauchy problem associated with three-dimensional Helmholtz-type equations, Appl. Math. Comput. 165(2005): 355-374.

[11] T. Belytschko, Y. Krongauz, D. Organ, M. Fleming, P. Krysl, Meshless methods: an overview and recent developments, Comput. Meth. Appl. Mech. Engrg. 139 (1996) 3-47.

[12] C.A. Duarte, J.T. Oden, H-p clouds – an h-p meshless method, Numer. Meth. Part. Diff. Eq. 12(1996) 673-705.

[13] W.K. Liu, Y. Chen, S. Jun, J.S. Chen, T. Belytschko, C. Pan, R.A. Uras, C.T. Chang, Overview and applications of the reproducing kernel particle methods. Arch. Comput. Meth. Engrg. 3(1996) 3–80.

[14] S.N. Atluri, S. Shen, The Meshless Local PetrovCGalerkin (MLPG) Method, Technical Science Press, Encino, 2002.

[15] E.J. Kansa, Multiquadric – A scattered data approximation scheme with applications to computational fluid dynamics II. Solutions to parabolic, hyperbolic, and elliptic partial differential equations, Comput. Math. Appl. 19(1990) 147-161.

[16] M.A. Golberg, C.S. Chen, The method of fundamental solution for potential, Helmholtz and diffusion problems, in: M.A. Golberg (Ed.), Boundary Integral Methods – Numerical and Mathematical Aspects, Computational Mechanics Publications, Southampton, 1998, 103-176.

[17] G. Fairweather, A. Karageorghis, The method of fundamental solutions for elliptic boundary value problems, Adv. Comput. Math. 9(1998) 69-95.

[18] K. Balakrishnan, P.A. Ramachandran, A particular solution Trefftz method for nonlinear Poisson problems in heat and mass transfer, J. Comput. Phys. 150(1999) 239-267.

[19] K. Balakrishnan, P.A. Ramachandran, The method of fundamental solutions for linear diffusion-reaction equations, Math. Comput. Model. 31(2000) 221-237.

[20] G.Fairweather, A. Karageorghis, P.A. Martin, The method of fundamental solutions for scattering and radiation problems, Engrg. Anal. Bound. Elem. 27(2003) 759-769.

[21] P.K. Kythe, Fundamental Solutions for Differential Operators and Applications, Birkháuser, Boston, 1996.

[22] P. Mitic, Y.F. Rashed, Convergence and stability of the method of meshless fundamental solutions using an array of randomly distributed source, Engrg. Anal. Bound. Elem. 28(2004) 143-153.

[23] T. Kitagawa, On the numerical stability of the method of fundamental solutions applied to the Dirichlet problem, Jpn. J. Appl. Math. 35(1988) 507-518.

[24] T. Kitagawa, Asymptotical stability of the fundamental solution method, J. Comput. Appl. Math. 38(1991) 263-269.

[25] R. Kress, Linear Integral Equations, Springer-Verlag, Berlin, 1989.

[26] P.C. Hansen, The truncated SVD as a method for regularization, BIT 27(1987) 534-553.

[27] H.W. Engl, Regularization methods for the stable solution of inverse problems, Surv. Math. Ind. 3(1993) 71-142.

[28] P.A. Ramachandran, Method of fundamental solutions: singular value decomposition analysis, Comm. Numer. Meth. Engrg. 18(2002) 789-801.

[29] B. Jin, A meshless method for the Laplace and biharmonic equations subjected to noisy boundary data, CMES-Comput. Model. Engrg. Sci. 6(2004) 253-261.

[30] P.C. Hansen, Analysis of discrete ill-posed problems by means of the Lcurve, SIAM Rev. 34(1992) 561-580.

[31] P.C. Hansen, D.P. O'Leary, The use of the L-curve in the regularization of discrete ill-posed problems, SIAM J. Sci. Comput. 14(1993) 1487-1503.

[32] G. Golub, M. Heath, G. Wahba, Generalized cross-validation as a method for choosing a good ridge parameter, Technometrics 21(1979) 215-223.

[33] C.L. Lawson, R.J. Hanson, Solving Least Squares Problems, Prentice-Hall, Englewood Cliff, 1974.

[34] H.W. Engl, W. Orever, Using the L-curve for determining optimal regularization parameters, Numer. Math. 69(1994) 25-31.

[35] C.R. Vogel, Non-convergence of the L-curve regularization parameter selection method, Inv. Prob. 12(1996) 535-547.

[36] A. Bogomolny, Fundamental solutions method for elliptic boundary value problems, SIAM J. Numer. Anal. 22(1985) 644-669.

[37] V.A. Kozlov, V.G. Mażya, A.V. Fomin, An iterative method for solving the Cauchy problem for elliptic equations, USSR Comput. Math. Math. Phys. 31(1992):45-52.

[38] R.T. Fenner, Source field superposition analysis of two-dimensional potential problems, Int. J. Numer. Meth. Engrg. 32(1991) 1079–1091.

[39] D. Nardini, C.A. Brebbia, A new approach for free vibration analysis using boundary elements, in: C.A. Brebbia (Ed.), Boundary Element Methods in Engineering, Springer, Berlin, 1982, 312-326.

[40] M. Hanke, P.C. Hansen, Regularization methods for large-scale problems, Surv. Math. Ind. 3(1993) 253-315.

[41] I. Saavedra, H. Power, Multipole fast algorithm for the least squares approach of the method of fundamental solutions for three-dimensional harmonic problems, Numer. Meth. Part. Diff. Eq. 19(2003) 828-845.
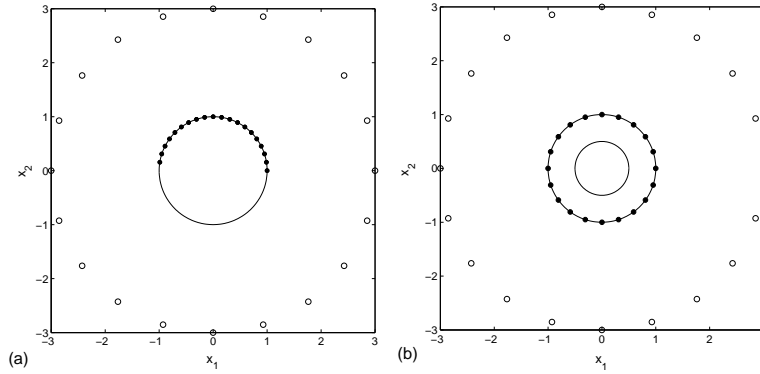
Fig. 1. Schematic illustration of the boundary $\partial\Omega$, distribution of boundary collocation points (dot) and source points (circle) for Ω and $\tilde{\Omega}$.
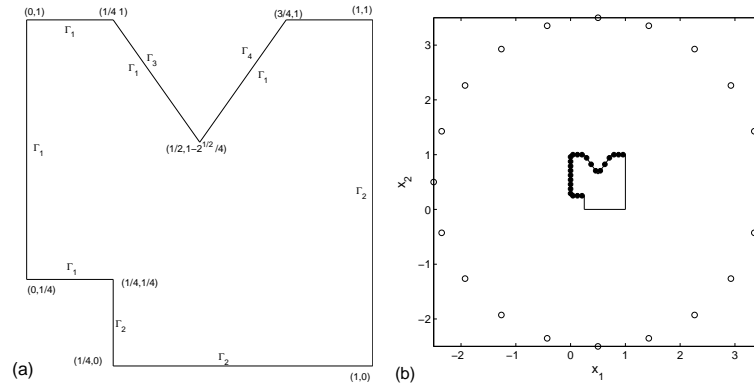
Fig. 2. Schematic illustration of the configuration of the complicated geometry $\hat{\Omega}$, and distribution of boundary collocation points (dot) and source points (circle).
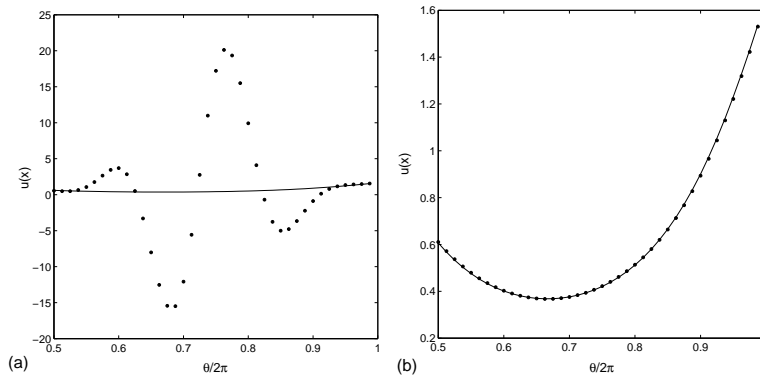
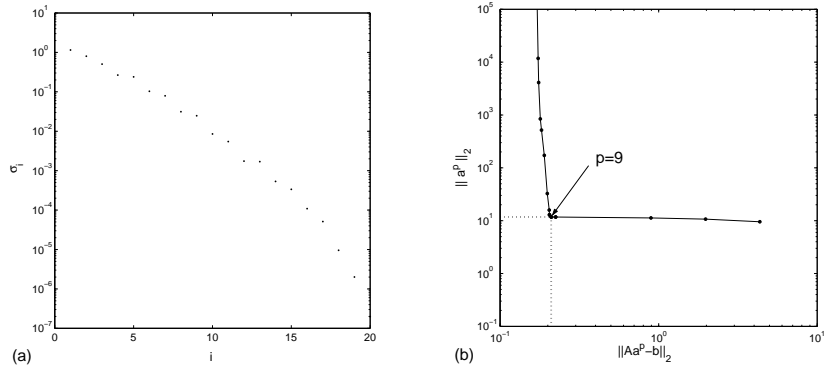Fig. 3. The retrieved $u(x)$ for Example 1 with 1% noise by (a) the least squares method and (b) the TSVD.

Fig. 4. The singular value spectrum of $\mathbf{A}$ for Example 1 and the L-curve.
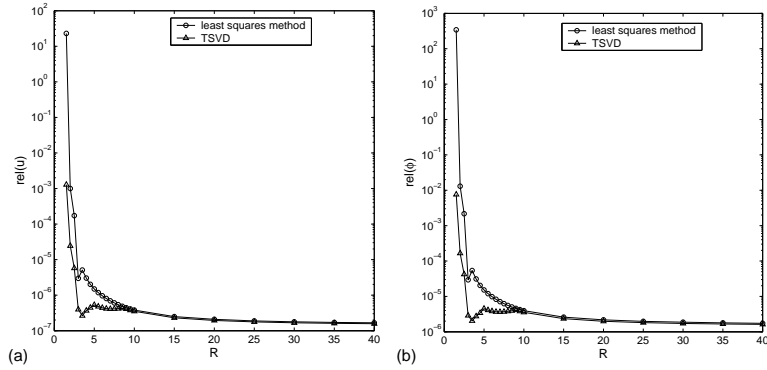
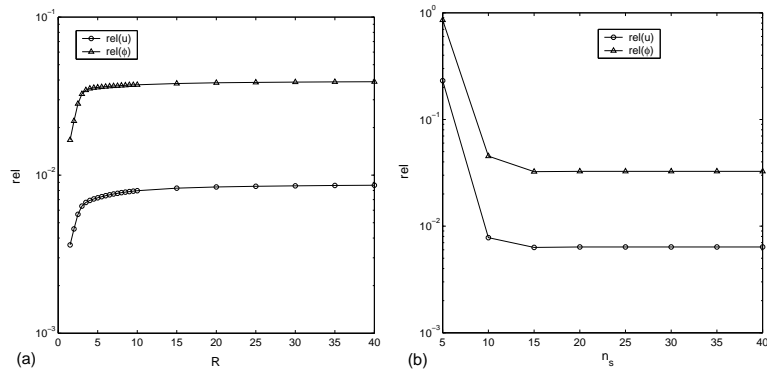Fig. 5. The accuracy variation of the numerical results with R for Example 1.

Fig. 6. The accuracy variation of the numerical results with respect to (a) R and (b) n_s for Example 1 with 1% noise.
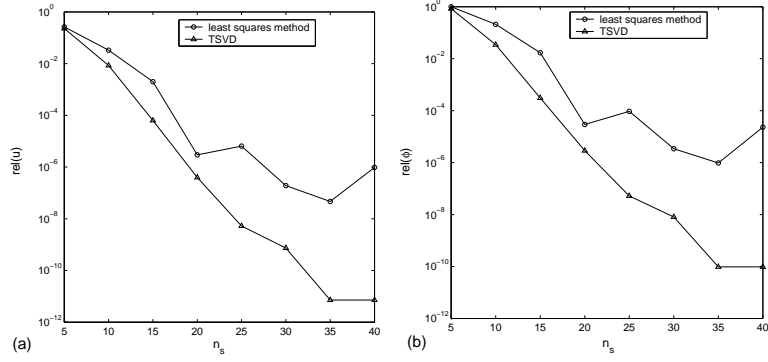
Fig. 7. The accuracy variation of the numerical results with respect to n_s for Example 1 with exact data.
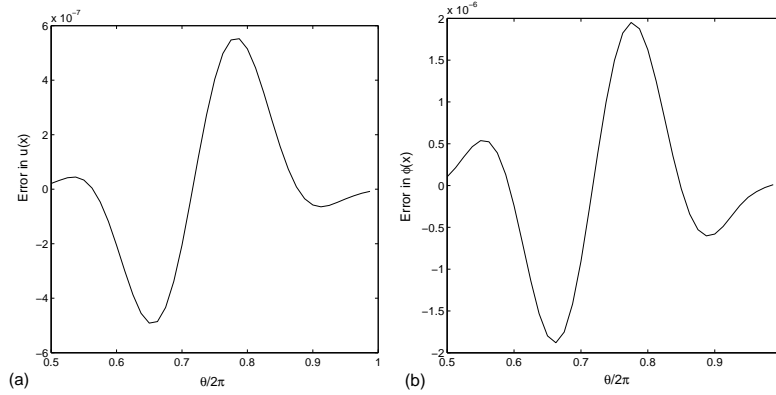

Fig. 8. Errors between the numerical and analytical solutions of Example 1 with exact data.
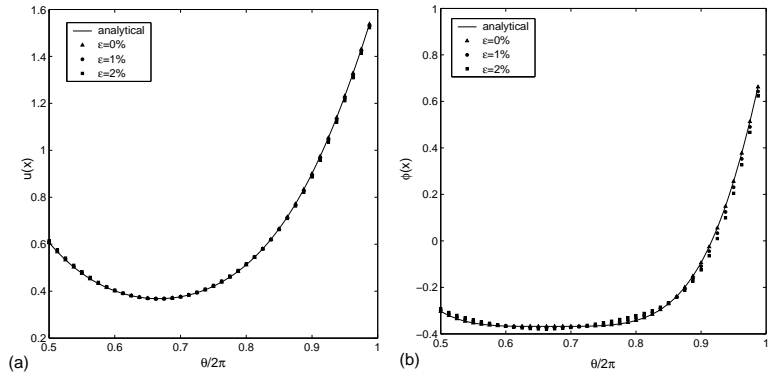

Fig. 9. The retrieved $u(x)$ and $\phi(x)$ for Example 1 with various levels of data noise.
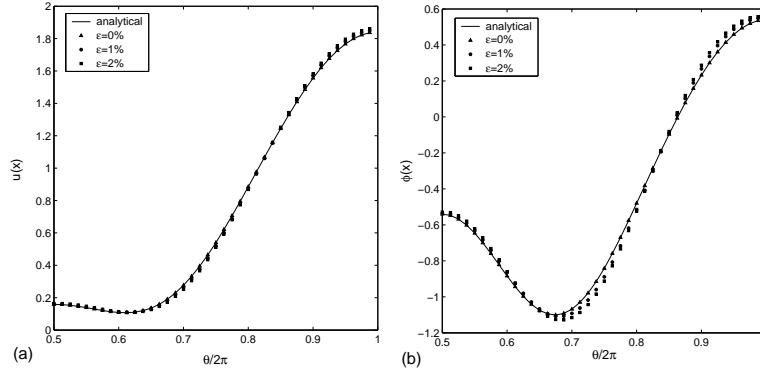
Fig. 10. The retrieved $u(x)$ and $\phi(x)$ for Example 2 with various levels of data noise.
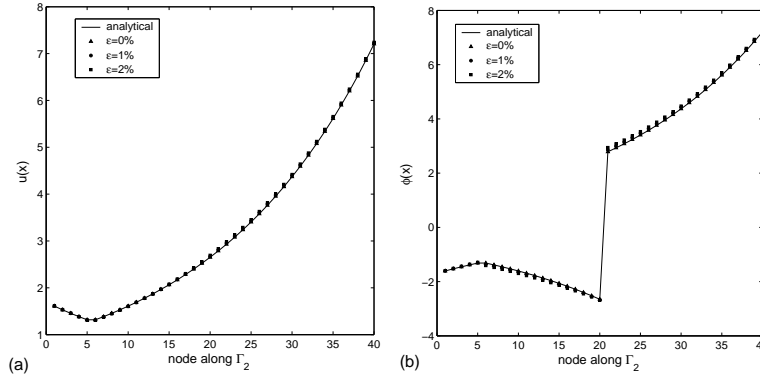

Fig. 11. The retrieved $u(x)$ and $\phi(x)$ for Example 3 with various levels of data noise.
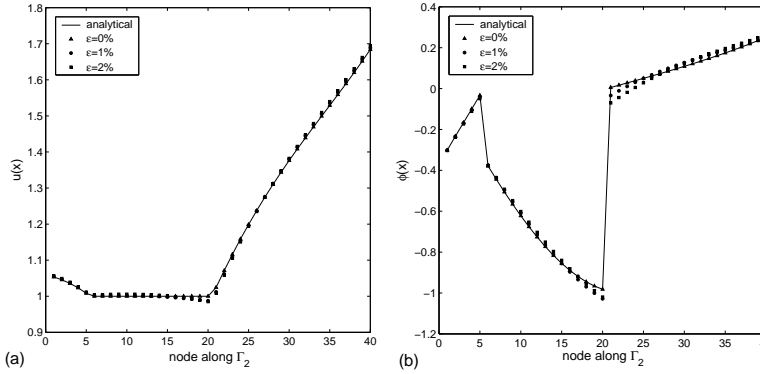

Fig. 12. The retrieved $u(x)$ and $\phi(x)$ for Example 4 with various levels of data noise.
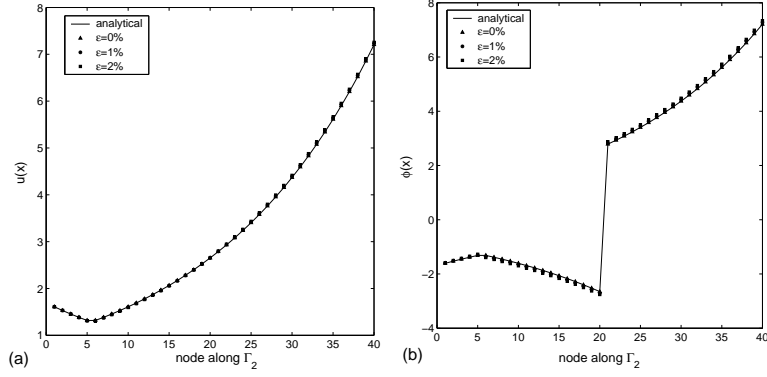
Fig. 13. The retrieved $u(x)$ and $\phi(x)$ for the modified version of Example 3 with various levels of data noise.
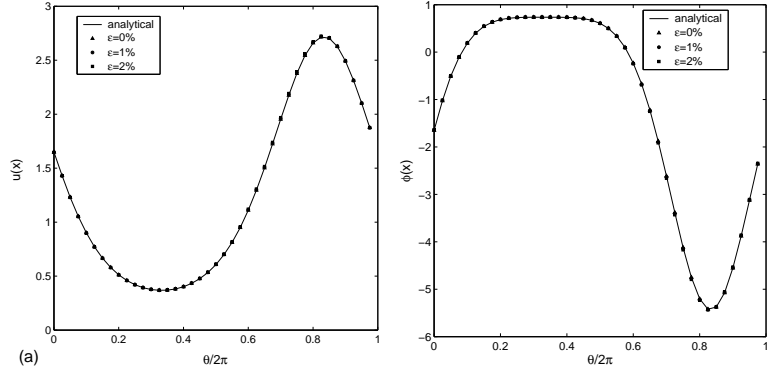

Fig. 14. The retrieved $u(x)$ and $\phi(x)$ for Example 5 with various levels of data noise.

Table 1
The results for examples with 2% data noise, where 3* stands for the modified version of Example 3.

Example	$Cond$	p	$rel(u)$	$rel(\phi)$
1	5.79×10^6	9	1.28×10^{-2}	6.66×10^{-2}
2	2.50×10^7	9	1.23×10^{-2}	2.91×10^{-2}
3	3.80×10^7	9	9.22×10^{-3}	2.46×10^{-2}
3*	3.63×10^7	9	8.22×10^{-3}	2.71×10^{-2}
4	7.13×10^8	10	6.30×10^{-3}	4.98×10^{-2}
5	6.61×10^2	15	4.84×10^{-2}	8.04×10^{-2}

24

Table 2
The results for Example 5 with exact data using various sets of source points.

$n_i + n_o$	$Cond$	$rel(u)$	$rel(\phi)$
10+10	4.61×10^3	Diverge	Diverge
8+12	1.02×10^3	1.62×10^{-3}	8.23×10^{-3}
4+16	4.10×10^3	3.28×10^{-7}	1.59×10^{-6}
0+20	6.61×10^2	6.28×10^{-8}	1.93×10^{-7}
2+20	1.35×10^4	1.14×10^{-7}	3.01×10^{-7}
4+20	1.91×10^4	2.78×10^{-7}	8.17×10^{-7}
8+20	2.70×10^4	1.70×10^{-6}	8.00×10^{-6}
12+20	3.31×10^5	1.17×10^{-5}	8.44×10^{-5}
16+20	8.02×10^5	2.23×10^{-5}	1.94×10^{-4}
20+20	1.71×10^7	3.30×10^{-5}	3.23×10^{-4}

Table 3
The results for Example 5 with 1% noise using various sets of source points.

$n_i + n_o$	p	$rel(u)$	$rel(\phi)$
8+12	19	5.49×10^{-2}	Diverge
4+16	15	1.10×10^{-2}	2.38×10^{-2}
0+20	15	2.42×10^{-3}	4.02×10^{-3}
2+20	15	3.79×10^{-3}	5.85×10^{-2}
4+20	18	1.09×10^{-2}	2.37×10^{-2}
8+20	20	Diverge	Diverge